ELSEVIER

Nuclear Instruments and Methods in Physics Research B 146 (1998) 557–564

NIM B
Beam Interactions with Materials & Atoms

High energy heavy ion irradiation damage in oxide superconductor $EuBa_2Cu_3O_y$

A. Iwase [a,*], N. Ishikawa [a], Y. Chimi [a], K. Tsuru [b], H. Wakana [c], O. Michikami [c], T. Kambara [d]

[a] *Japan Atomic Energy Research Institute (JAERI), Naka-gun, Tokai-Mura, Ibaraki 319-1195, Japan*
[b] *Information Hardware Systems Laboratory, NTT Integrated Information & Energy Systems Laboratories, Musashino-shi, Tokyo, 180-0012, Japan*
[c] *Faculty of Engineering, Iwate University, Morioka-shi, Iwate 020-0066 Japan*
[d] *Atomic Physics Laboratory, The Institute of Physical and Chemical Research (RIKEN), Wako-shi, Saitama, 351-0198, Japan*

Abstract

Defect production and recovery are studied in oxide superconductor, $EuBa_2Cu_3O_y$, irradiated with high energy (80 MeV–3.80 GeV) heavy ions. X-ray diffraction measurements show that the *c*-axis lattice parameter increases linearly with increasing ion-fluence. The rate of the increase in lattice parameter can be scaled with the primary ionization rate, dJ/dx, and not with the electronic stopping power, S_e. This result implies that a Coulomb explosion process triggers the atomic displacements in $EuBa_2Cu_3O_y$. From the electrical resistivity change at 100 K as a function of ion-fluence, the diameter and the resistivity of a cylindrically-shaped damage region can be determined. Irradiation induced resistivity change is markedly recovered during the annealing of the specimen up to 300 K. The dJ/dx dependence of the diameter and the resistivity of damaged region is discussed.

Keywords: Oxide superconductors; Defect production; Electronic excitation; Primary ionization rate; X-ray diffraction measurement; Resistivity measurement

1. Introduction

In oxide superconductors, it is well known that a highly damaged region is produced along the path of swift heavy ions [1]. As such "columnar defects" can effectively pin the quantized magnetic flux and are quite useful for the enhancement of superconducting critical current density, the effects of these defects on the superconducting properties have been extensively studied [2]. As the defects are produced continuously along the ion beam path, and only high energy heavy ions can produce them, it has been believed that the high density electronic excitation induced by high energy heavy ions produces the columnar defects in oxide superconductors. However, the mechanism through which the energy of excited electrons is transferred to the target atoms has never been fully understood.

* Corresponding author. Tel.: +81 29 282 5470; fax: +81 29 282 6716; e-mail: iwase@popsvr.tokai.jaeri.go.jp

0168-583X/98/$ – see front matter
PII: S0168-583X(98)00446-7

In this paper, we summarize our recent experimental results on the defect production in Eu-$Ba_2Cu_3O_y$ oxide superconductors irradiated with 80 MeV–3.80 GeV heavy ions [3–5], and then discuss the defect production mechanism.

2. Experimental procedure

2.1. Specimens

Thin films of $EuBa_2Cu_3O_y$ (called EBCO-film hereafter) were prepared on MgO substrates by means of rf magnetron sputtering [6]. The films were *c*-axis oriented and the thickness was about 300 nm. The superconducting transition temperature, T_c, was 80–89 K.

2.2. Irradiation at room temperature, and measurements of the X-ray diffraction pattern

The EBCO-films were irradiated parallel to the *c*-axis at room temperature with the following ions; 120 MeV $^{35}Cl^{8+}$, 90 MeV $^{58}Ni^{6+}$, 200 MeV $^{58}Ni^{12+}$, 125 MeV $^{79}Br^{10+}$, 80 MeV $^{127}I^{7+}$, 200 MeV $^{127}I^{12+}$, and 120 MeV $^{197}Au^{10+}$ from the tandem accelerator at JAERI (Japan Atomic Energy Research Institute)-Tokai, and 3.54 GeV $^{136}Xe^{31+}$ and 3.80 GeV $^{181}Ta^{37+}$ from the ring cyclotron at RIKEN (The institute of Physical and Chemical Research).

For the data analysis mentioned below, it is necessary to confirm that the charge state of ions in the specimen has become the equilibrium state, Z^*. Therefore, some specimens were covered with thin Al foils (3 μm thick) when they were irradiated. By having the ion beam first penetrate a thin foil, the equilibrium charge state beams can be prepared.

To estimate the effect of elastic interaction between ions and the target atoms, low energy ion irradiations (0.85 MeV $^4He^+$, 1.0 MeV $^{12}C^+$, 0.95 MeV $^{20}Ne^+$ and 2 MeV $^{40}Ar^{2+}$) were also performed by using a 2 MV VdG accelerator at JAERI-Tokai.

Since the projected ranges for all irradiations were much larger than the specimen thickness, the energy loss of ions in the specimen was much smaller than the initial ion energy, and the irradiating ions did not remain in the specimen as impurities. Before and after irradiations, the X-ray (Cu Kα) diffraction patterns were measured. From the shift of the Bragg peaks, we estimated the *c*-axis lattice parameter change by ion-irradiation.

2.3. Electrical resistivity measurements at 100 K as a function of ion-fluence

EBCO-films were irradiated with energetic ions at 100 K. Irradiating ions were almost the same as for X-ray diffraction measurements. The electrical resistivity was measured at 100 K as a function of ion-fluence by using a conventional four probe method. In order to study the recovery behavior of the irradiation effects, the specimens were annealed up to 300 K after irradiations, and then cooled again to <100 K. During the annealing and cooling processes, the resistivity was measured as a function of specimen temperature.

3. Results and discussion

3.1. C-axis lattice parameter increase by high energy ion irradiation

Fig. 1 displays the relative increase in the *c*-axis lattice parameter, $\Delta c/c_0$, as a function of ion-fluence, Φ, where c_0 is the *c*-axis parameter before irradiation and Δc the increment of the lattice parameter by irradiation. For clarity, not all the data are shown in the figure. The values of $\Delta c/c_0$ change linearly against the ion-fluence. The linear Φ dependence of $\Delta c/c_0$ was also observed for low energy (∼1 MeV) ion irradiations and the lattice parameter increase per unit fluence, $(\Delta c/c_0)/\Phi$, is proportional to the nuclear stopping power, S_n [3]. This means that for low energy ion irradiations, the elastic collisions between the ions and target atoms cause the lattice parameter increment. On the other hand, for high energy ion irradiation, which excites electrons densely along the ion beam path, the values of $(\Delta c/c_0)/\Phi$ are much larger than for low energy ions at the same S_n. From these results, we can conclude that the *c*-axis lattice

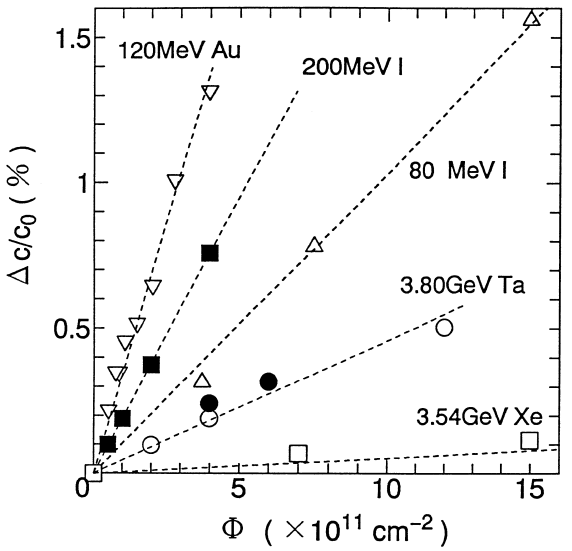

Fig. 1. Values of ($\Delta c/c_0$) as a function of ion-fluence for EBCO-film irradiated with high energy heavy ions. For 3.8 GeV Ta^{37+} irradiation, (●) data for the specimens covered with Al foil, and (○) for the specimens without Al foil.

parameter increase observed in EBCO-film irradiated with high energy ions is caused by the high density electron excitation.

In Fig. 1 the result for the specimens covered with Al foils (solid circles) is compared with that without Al foils (open circles) for 3.80 GeV Ta^{37+} irradiations. Data points for the specimens with and without Al foils lie on the same line. This means that even without Al foil, the charge state of ions becomes the equilibrium state instantaneously when the ion beam enters the specimen.

To describe the effect of electron excitation, the electronic stopping power, S_e, has often been used as a scaling parameter. The irradiation effect on the c-axis lattice parameter, however, cannot be described only by the S_e values. As can be seen in Fig. 2, the comparison of lattice parameter changes for the same S_e values shows that lower velocity ion irradiations produce larger effect. Similar dependence of irradiation effect on ion velocity has been observed in the insulator $Y_3Fe_5O_{12}$ [7] and pure bismuth [8].

In order to account for this "velocity effect", we use the primary ionization rate, dJ/dx, as a scaling parameter instead of S_e. The quantity dJ/dx is the

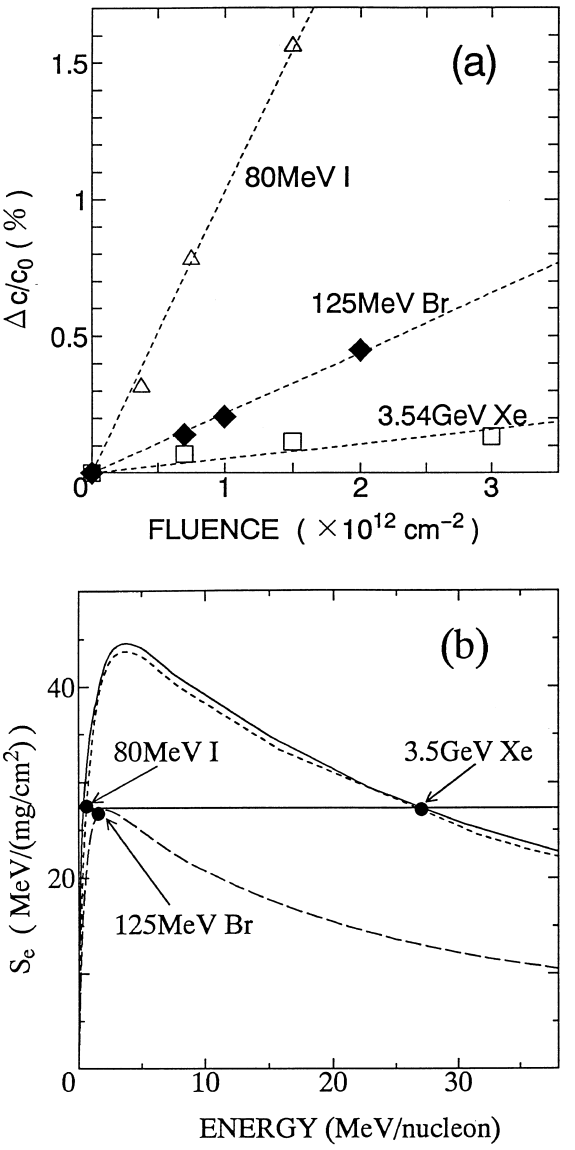

Fig. 2. (a) Values of ($\Delta c/c_0$) as a function of ion-fluence for 80 MeV I, 125 MeV Br and 3.54 GeV Xe irradiations. (b) Stopping power for I, Br and Xe ions as a function of ion energy per atomic mass unit.

number of primarily ionized atoms per unit length of ion path, and is given by [9,10],

$$dJ/dx = (\alpha Z^{*2}/I_0\beta^2) \times [\ln\{2mc^2\beta^2/(1-\beta^2)I_0\} - \beta^2 + 3.04], \quad (1)$$

where Z^* is the equilibrium charge of the irradiating ion in the target [11], β the ion velocity divided by the velocity of light, c, I_0 the ionization energy of most loosely bound electrons of a target, and m the electron mass. In Eq. (1), the values of α and I_0 depend on the target material. We adopt $I_0 = 10$ eV, which is the average value of the first ionization energy for atoms composing the EBCO-film. Since it is quite difficult to estimate the value of α, the units of dJ/dx remain arbitrary here. Fig. 3 displays the c-axis lattice parameter change per unit ion fluence, $(\Delta c/c_0)/\Phi$, as a function of dJ/dx. The values of $(\Delta c/c_0)/\Phi$ are well scaled by dJ/dx and are proportional to $(dJ/dx)^4$.

Vineyard [12], and Johnson and Evatt [13] have treated the effect of energy deposited instantaneously in a very small cylindrical region of solid target by using the laws of classical heat conduction in a continuum. This "thermal spike model" shows that the total number of atomic displacements per unit length of the spike, η, is

$$\eta \propto \varepsilon^2, \tag{2}$$

where, ε is the energy deposited per unit cylindrical spike. If the thermal spike is energized by the mutual repulsion of primarily ionized atoms (often called "Coulomb explosion process"), the repulsive energy density in a cylindrical region along the ion path is [14],

$$\varepsilon_{\text{coulomb}} \propto (dJ/dx)^2. \tag{3}$$

Substituting $\varepsilon_{\text{coulomb}}$ into Eq. (2), the number of displaced atoms per unit ion path length is given by,

$$\eta \propto (dJ/dx)^4. \tag{4}$$

This dependence of irradiation effect on dJ/dx is the same as the present experimental result (Fig. 3). Therefore, we can at least qualitatively explain the mechanism of high energy heavy ion irradiation effect on the lattice parameter in EBCO-film as follows; the energies of electrons densely excited by ions are transferred to target atoms through the Coulomb explosion process, then energize a thermal spike, resulting in atomic displacements in the EBCO-film.

It should be noted here that Seiberling et al. have observed the linear $(dJ/dx)^4$ dependence of the sputtering yield in UF_4 irradiated with heavy ions, and have explained the result in the similar manner as presented above [15,16].

3.2. Electrical resistivity change at 100 K by high energy heavy ion irradiation

Fig. 4 displays the ion-fluence dependence of $\Delta\rho/\rho_0$ for EBCO-film irradiated with 80 MeV–3.54 GeV heavy ions at 100 K, where $\Delta\rho$ is the resistivity change by irradiation and ρ_0 the resistivity at 100 K before irradiation. To estimate the effect of the elastic collision between the irradiating ions and target atoms on the resistivity, we also performed the low energy (~1 MeV) ion irradiation experiments [17]. The result shows that the resistivity changes per unit fluence, $(\Delta\rho/\rho_0)/\Phi$, for low energy irradiations are very small, and the electronic excitation dominantly contributes to the resistivity changes for high energy heavy ions shown in Fig. 4.

Fig. 5 gives the comparison of the resistivity change for the same S_e values. Even at the same S_e, lower velocity ion irradiation produces larger change in the resistivity. This trend is the same as for the lattice parameter change.

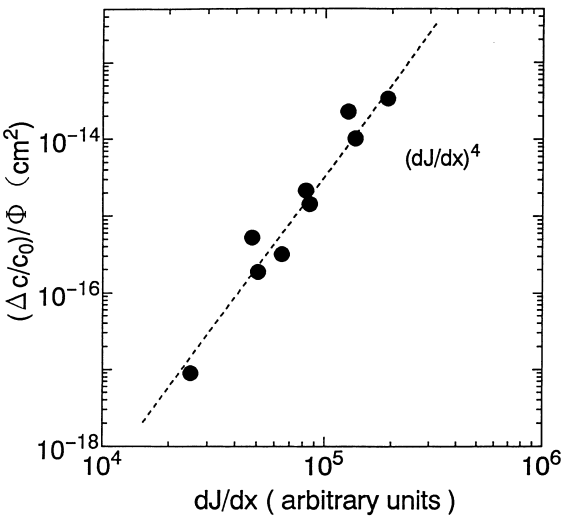

Fig. 3. Values of $(\Delta c/c_0)/\Phi$ as a function of dJ/dx. Dotted line represents the line proportional to $(dJ/dx)^4$.

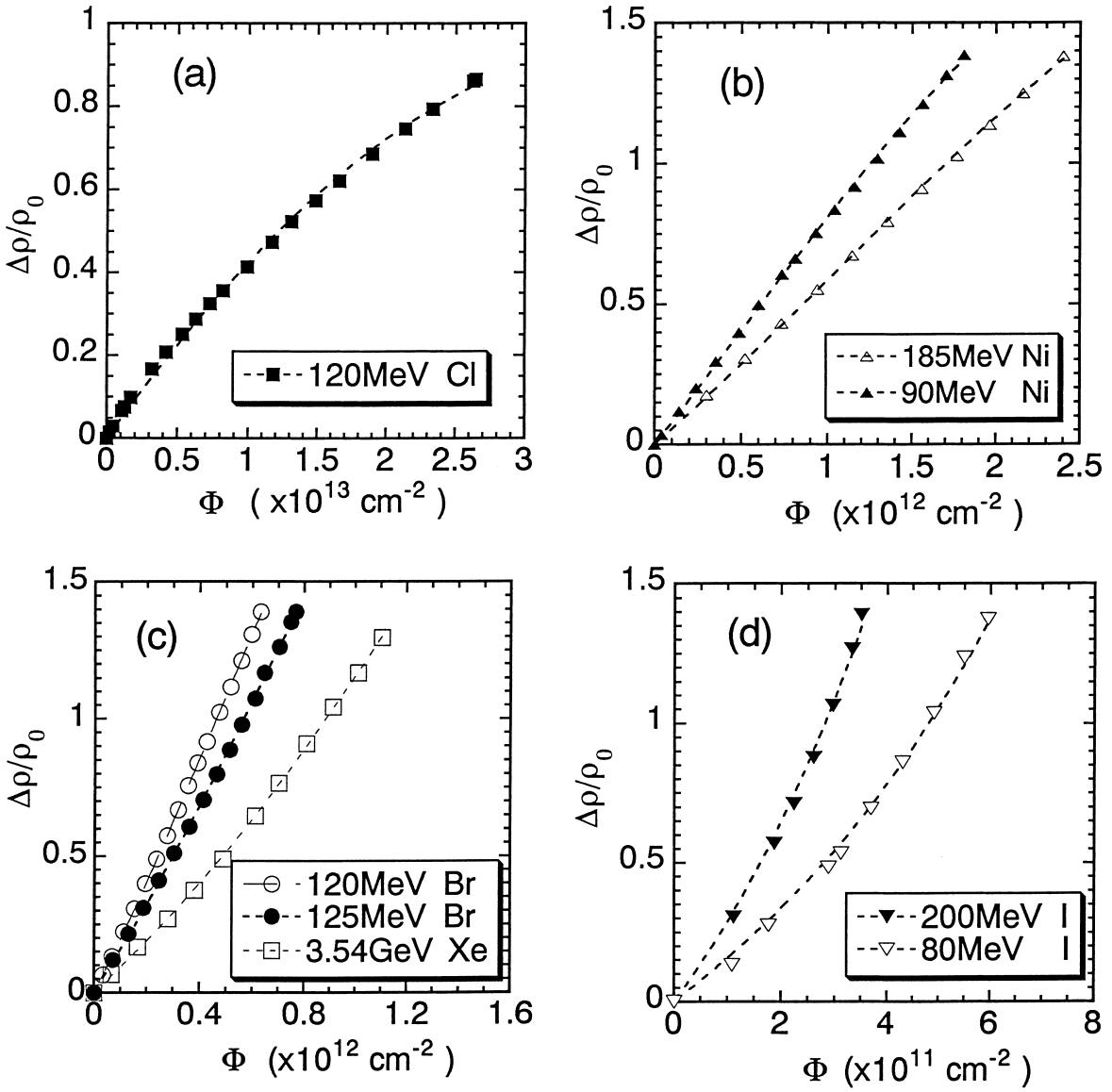

Fig. 4. Ion-fluence dependence of $\Delta\rho/\rho_0$ for EBCO-film irradiated with high energy heavy ions.

The shapes of $(\Delta\rho/\rho_0)-\Phi$ curve strongly depend on the irradiating ions. They are concave for Xe, Br, and I ions, and are convex for Cl and Ni ions. For high energy heavy ion irradiations, the production of the cylindrical damage region along the ion beam path can be expected. Rayleigh has calculated the electrical conductivity of a solid including randomly distributed parallel cylinders in the dilute case (volume fraction of cylinders, $\delta \ll 1$), where the conductivity inside the cylinder is different from its outside [18]. By using the renormalization method of Bruggeman [19], Klaumünzer has extended the Rayleigh's formula to arbitrary values of $\delta < 1$ [20]. The final formula which can be applied to the resistivity of the specimen irradiated with high energy heavy ions is given by,

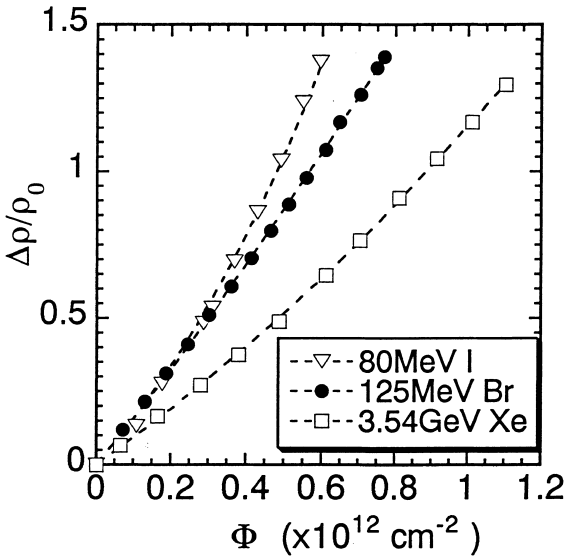

Fig. 5. Ion-fluence dependence of $\Delta\rho/\rho_0$ for EBCO-film irradiated with 80 MeV I, 125 MeV Br and 3.54 GeV Xe ions. Values of electronic stopping power for these three irradiations are the same ($S_e = 27$ MeV/(mg/cm^2)), See Fig. 2(b)).

$$\left(\frac{\rho(\Phi)-\rho'}{\rho_0-\rho'}\right)\sqrt{\frac{\rho_0}{\rho(\Phi)}} = \left(\frac{(\rho(\Phi)/\rho_0)-k}{1-k}\right)\sqrt{\frac{\rho_0}{\rho(\Phi)}} = 1-\delta, \quad (5)$$

where ρ_0 is the electrical resistivity of the undamaged region, ρ' the resistivity inside the cylindrical damage region, $k = \rho'/\rho_0$, and $\rho(\Phi)$ the resistivity of the irradiated specimen, which is measured perpendicular to the cylinder axis. The volume fraction of damaged region, δ, is,

$$\delta = 1 - \exp(-A\Phi), \quad (6)$$

where $A = \pi D^2/4$ is the cross section of a damaged region and D is its diameter. Next, we analyze the experimental $\Delta\rho/\rho_0 - \Phi$ curves shown in Fig. 4 using Eqs. (5) and (6). There are two fitting parameters, A (or D) and k in Eqs. (5) and (6). The fit was carried out using the usual least-squares method. The dotted lines of Fig. 4 represent the best fit to the experimental curves.

In Fig. 6, the values of adjustable parameters, D and k are plotted against dJ/dx. The dependence of the diameter, D, on dJ/dx is rather weak. Except for Cl ion irradiation, the values of D are 10 ± 2 nm for all irradiations. The values of k, however,

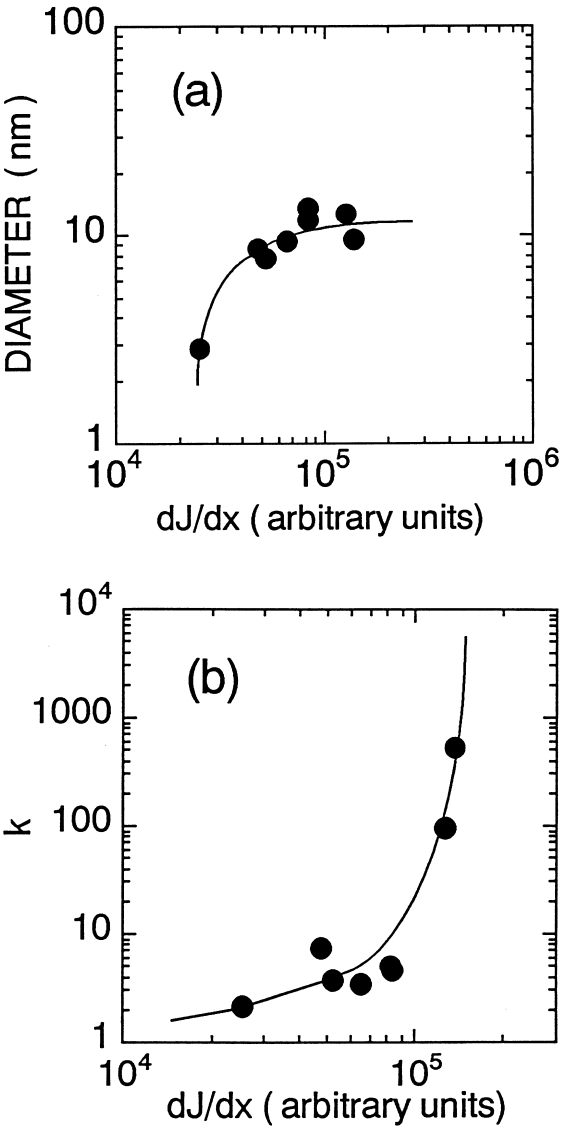

Fig. 6. (a) Diameter of the damaged region as a function of dJ/dx. (b) Ratio of the resistivity inside the damaged region to that of undamaged region, k, as a function of dJ/dx.

strongly depend on dJ/dx, and tend to diverge at large dJ/dx values. The electronic stopping power, S_e, is not a good parameter for describing the cylindrical damage produced by swift heavy ions because at the same S_e, the value of k for 80 MeV I ions is more than ~50 times larger than for 3.5 GeV Xe ions.

Finally, we compare the present results with those from transmission electron microscope (TEM) observations. TEM observations show that cylindrically amorphized regions are produced in oxide superconductors irradiated with swift heavy ions when the value of S_e is above a threshold. The diameters of the damaged region determined by the present resistivity measurements at 100 K are, however, larger than those of the amorphized region observed by TEM at room temperature. This difference is partly attributed to the existence of defect recovery below room temperature [21]. As can be seen in Fig. 7, 50–70% of damage produced at 100 K is recovered during the subsequent annealing up to 300 K. Another reason for the difference in the damaged region diameter for the two kinds of measurements is as follows; TEM usually observes only the amorphized region, while the present resistivity measurement can detect not only the amorphized region but also the more softly damaged region which may distribute around the amorphized region. By using Eq. (5), we can determine the diameter, D, and the resistivity ratio, k, even when the S_e values of irradiating ion are below the threshold, and the value of k is less than 10. This result means that such a softly damaged region is produced along the ion beam path also when the value of S_e is below the threshold for amorphized track production.

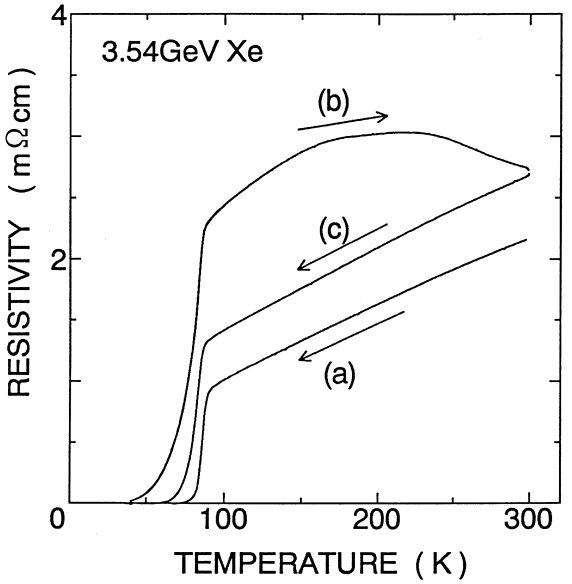

Fig. 7. Resistivity–temperature curves for EBCO-film measured (a) before irradiation, (b) during warming up to 300 K after irradiation with 3.54 GeV Xe ions at 100 k, and (c) during the subsequent cooling down to <100 K.

4. Summary

The effects of high energy heavy ion irradiation in EBCO-film have been studied by measuring the c-axis lattice parameter change at room temperature and the electrical resistivity change at 100 K. We have found that the primary ionization rate, dJ/dx, is much better than the electronic stopping power, S_e, for describing the irradiation effects in EBCO. The lattice parameter change per unit ion-fluence, $(\Delta c/c_0)/\Phi$, is proportional to $(dJ/dx)^4$. This result implies that the atomic displacements are induced in EBCO-film through the thermal spike energized by the Coulomb explosion process. From the dependence of the electrical resistivity on the ion-fluence, the diameter and the resistivity of the cylindrical damage region along the ion path have been determined. The dependence of the damaged region diameter on dJ/dx is weak, while the ratio of the resistivity inside the damaged region to that of the undamaged region tends to diverge with increasing dJ/dx.

Acknowledgements

The authors would like to thank the technical staffs of the Accelerators Division at JAERI and of RIKEN Accelerator Facility for their great help.

References

[1] B. Hensel, J. Nucl. Mater. 251 (1997) 218, and references therein.
[2] G. Blatter, M.V. Feigel'man, V.B. Geshkenbein, A.I. Larkin, V.M. Vinokur, Rev. Mod. Phys. 66 (1994) 1125.
[3] N. Ishikawa, A. Iwase, Y. Chimi, H. Maeta, K. Tsuru, O. Michikami, Physica C 259 (1996) 54.
[4] N. Ishikawa, Y. Chimi, A. Iwase, H. Maeta, K. Tsuru, O. Michikami, T. Kambara, T. Mitamura, Y. Awaya, M. Terasawa, Nucl. Instr. and Meth. B 135 (1998) 184.

[5] N. Ishikawa, Y. Chimi, A. Iwase, K. Tsuru, O. Michikami, Mat. Res. Soc. Symp. Proc., in press.
[6] O. Michikami, M. Asahi, H. Asano, Jpn. J. Appl. Phys. 29 (1990) L298.
[7] M. Toulemonde, S. Bouffard, F. Studer, Nucl. Instr. Meth. B 91 (1994) 108.
[8] Z.G. Wang, Ch. Dufour, B. Cabeau, J. Dural, G. Fuchs, E. Paumier, F. Pawlak, M. Toulemonde, Nucl. Instr. Meth. B 107 (1996) 175.
[9] H. Bethe, Ann. Phys. 5 (1930) 325.
[10] R.L. Fleisher, P.B. Price, R.M. Walker, Nuclear Tracks in Solids, University of California Press, Berkeley CA, 1975.
[11] T.E. Pierce, M. Blann, Phys. Rev. 173 (1968) 390.
[12] G.H. Vineyard, Rad. Eff. 29 (1976) 245.
[13] R.E. Johnson, R. Evatt, Rad. Eff. 52 (1980) 187.
[14] R.E. Johnson, J. Schou, Kgl. Danske Vidensk. Selsk. mat.-fis. Medd. 43 (1993) 403.
[15] L.E. Seiberling, J.E. Griffith, T.A. Tombrello, Rad. Eff. 52 (1980) 201.
[16] L.E. Seiberling, C.K. Meins, B.H. Cooper, J.E. Griffith, M.H. Mendenhall, T.A. Tombrello, Nucl. Instr. and Meth. 198 (1982) 17.
[17] N. Ishikawa, Y. Chimi, A. Iwase, K. Tsuru and O. Michikami, J. Nucl. Mater. in press.
[18] J.W. Rayleigh, Phil. Mag. 34 (1892) 481.
[19] D.A.G. Bruggeman, Ann. Phys. 24 (1935) 636.
[20] S. Klaumünzer, Rad. Eff. Defects in Solids 126 (1993) 141.
[21] Y. Zhu, Z.X. Cai, R.C. Budhani, M. Suenaga, D.O. Welch, Phys. Rev. B 48 (1993) 6436.